A model adaptive and model reduction strategy combining system-theoretical methods and substructuring

Christian Rickelt, Stefanie Reese, Department of Civil Engineering,
Ruhr University Bochum, 44780 Bochum,Germany
(rickelt,reese)@nm.ruhr-uni-bochum.de

Summary
This paper focuses on a new three-level discretisation strategy which enables the transition between continuum/structural (I) and structural/black box modelling (II). The transition (I) is realised by means of a model adaptive concept based on an innovative finite element technology. For transition (II) we apply the truncated balanced realisation method (TBR). The latter represents an established system theoretical model reduction technique which is here combined with a novel substructure technique. The approach provides a modular concept to facilitate the computational analysis of complex structures. The final goal is to apply the strategy to life time estimation.

1 Introduction
In spite of the progress achieved in hardware and software development it is still a very challenging task to compute the behaviour of a building over its entire life span. In order to make such a computation possible not every part of the structure can be modelled with the highest accuracy. However, it is certainly difficult to decide which level of modelling should be assigned to the different building components.

To this end the structure is at first divided into subsystems. Only if damage has occurred in one unit (which could have been detected e.g. by means of a suitable monitoring method) it is modelled at the continuum level which represents the finest discretisation scale. The elastic zones of the damaged construction units are discretised by structural elements. The third modelling level consists of so-called dynamically equivalent “black box” models to be generated via system theoretical modal reduction methods. An overview about different methods is given by (Antoulas, Sorensen and Gugerin 2001). A difficulty of the approach lies in the fact that it is not known beforehand which parts of the structure have to be modeled as black box or as continuum. In addition the loading situation in the building is subject to steady changes over life time, therefore also the substructuring should be flexible. For this reason it is necessary to automate the procedure. Similar approaches, to connect model reduction and substructure techniques have been investigated by e.g. (Barbone, Givoli and Patlashenko 2003), (Soize 2003) and (Petersmann 1986).

The first part of the paper concentrates on a new strain-based model adaptive concept which uses besides the concept of “hanging nodes” the advantages of the Q1SP element family (Reese 2003, Reese 2004). The principle ideas and properties of the element formulation are summed up briefly. The second part of this paper focuses on a combination of the proposed substructure technique with the well-known system theoretical model reduction technique TBR. The paper is completed by a presentation and interpretation of the obtained results.

2 Model adaptivity
The transition between the continuum and the structural level is carried out by means of a model adaptive concept which exploits on the one hand the so-called hanging node concept and on the other hand the characteristic properties of the Q1SP element family. In dependence of the way

how the stress-strain relation is evaluated inside the element, Q1SP can play the role of classical 3D (continuum), (solid) shell or beam elements. However, independently of the chosen type the element possesses eight nodes and three nodal displacement degrees-of-freedom. It is therefore possible to discretise a structure with arbitrarily many elements over the thickness or to couple the continuum type with the shell type, according to a previously defined accuracy criterion. Here a strain-based criterion is used which allows us to make a judgement about the amount of warping in the structure. The stronger the warping the more elements are needed over the thickness.

2.1 Element technology

It has been discovered already in the seventies that classical bi-linear or tri-linear displacement-based isoparametric finite element formulations exhibit the undesirable effect of "locking". In the past various methods have been developed to overcome the problem. One of them is the method of incompatible modes where the uncomplete ansatz space is enriched with the missing terms. The additional modes lead to an overlapping of the element edges (incompatibility). Obviously such incompatible modes cannot be chosen arbitrarily. One usually requires that they do not introduce any additional energy into the system. In this way an additional relation to determine the so-called internal element degrees-of-freedom (related to the incompatible modes) is derived.

A sound mathematical basis for this kind of element technology has been presented by (Simo and Rifai 1990) and (Simo and Armero 1992). Since then it is termed "enhanced strain method". However, in the regime of large deformations (Wriggers and Reese 1996) detected numerical instabilities (hourglassing) in areas of large compression, a problem which has still not been solved. Partially for this reason several authors went back to the concept of reduced integration with hourglass stabilization originally suggested by Belytschko and coworkers ((Belytschko et al. 1984), (Belytschko and Bachrach 1986), (Belytschko and Bindeman 1993)). Recent approaches of this kind can be found in (Puso 2000), (Cardoso et al. 2002) and (Legay and Combescure 2003). One of the crucial points of these new formulations is the fact that the hourglass stabilization is physically based. Additionally it is possible to choose a form which is by definition positive definite. In this way hourglass instabilities are avoided. The concept of (Reese 2004) has the extra advantage that, as already mentioned, it can be transferred into a 3D, solid-shell or solid-beam element. There is neither a kinematical assumption nor any simplification of the continuum material modelling necessary.

The point of departure is the two-field variational functional upon which also the classical non-linear enhanced strain method (see e.g. Simo & Armero 1992) is based. Besides the displacement vector, the so-called enhanced (incompatible) strain $\mathbf{H}^{\mathrm{h}}_{\mathrm{enh}}$ is introduced which acts as additional independent variable. The two equations of weak form read

$$\mathrm{g}_1(\mathbf{u}^{\mathrm{h}}, \mathbf{H}^{\mathrm{h}}_{\mathrm{enh}}) = \int_{\mathrm{B}^{\mathrm{h}}_0} \mathbf{P}^{\mathrm{h}} : \mathrm{Grad}\,\mathrm{d}\mathbf{u}^{\mathrm{h}}\, dV - \mathrm{g}_{\mathrm{a}} = 0\,, \qquad \mathrm{g}_2(\mathbf{u}^{\mathrm{h}}, \mathbf{H}^{\mathrm{h}}_{\mathrm{enh}}) = \int_{\mathrm{B}^{\mathrm{h}}_0} \mathbf{P}^{\mathrm{h}} : \mathrm{d}\mathbf{H}^{\mathrm{h}}_{\mathrm{enh}}\, dV = 0 \tag{1}$$

where the first Piola-Kirchhoff stress tensor $\mathbf{P}^{\mathrm{h}} = \mathbf{P}(\mathbf{H}^{\mathrm{h}}, (\mathbf{Z}^{\mathrm{h}}_{\mathrm{i}}, \mathrm{i} = 1, \ldots, \mathrm{n})) = \widetilde{\mathbf{P}}(\mathbf{H}^{\mathrm{h}})$ is displayed as a function of the physical (total) strains $\mathbf{H}^{\mathrm{h}}$ and the history variables $\mathbf{Z}^{\mathrm{h}}$. The index "h" indicates quantities which are evaluated by means of a discretisation in space or in time. The strain $\mathbf{H}^{\mathrm{h}}$ (which is additively split into a compatible and an enhanced, i. e. incompatible, part) is interpolated in a similar way as proposed by (Simo and Armero 1992):

$$\boldsymbol{H}^{\mathrm{h}} = \left(\boldsymbol{B}_{\mathrm{lin}} + \left(\boldsymbol{j}^{1}_{0}\, \boldsymbol{L}^{1}_{\mathrm{hg}} + \boldsymbol{j}^{2}_{0}\, \boldsymbol{L}^{2}_{\mathrm{hg}}\right)\boldsymbol{M}_{\mathrm{hg}}\right)\boldsymbol{U}_{\mathrm{e}} + \boldsymbol{j}^{1}_{0}\, \boldsymbol{L}_{\mathrm{enh}}\, \boldsymbol{W}_{\mathrm{e}} = \boldsymbol{H}^{\mathrm{h}}_{\mathrm{comp}} + \boldsymbol{H}^{\mathrm{h}}_{\mathrm{enh}} \tag{2}$$

From now on matrix notation is used, with matrices and vectors denoted by bold italic letters. In the latter relation $\boldsymbol{B}_{\mathrm{lin}}$ represents the constant part of the classical $\boldsymbol{B}$ matrix. The matrices $\boldsymbol{j}^{1}_{0}$ and $\boldsymbol{j}^{2}_{0}$ include components of the inverse Jacobi matrix. $\boldsymbol{L}^{1}_{\mathrm{hg}}$ and $\boldsymbol{L}^{2}_{\mathrm{hg}}$ are functions of the

local convective coordinates ξ,η,ζ and $\boldsymbol{M}_{\mathrm{hg}}$ contains the so-called stabilisation vectors. The physical and the internal degrees-of-freedom are represented by $\boldsymbol{U}_{\mathrm{e}}$ and $\boldsymbol{W}_{\mathrm{e}}$, respectively.

One of the principle ideas of the Q1SP element family is to develop the first Piola-Kichhoff stress tensor into a Taylor expansion which is in the case of the 3D element formulated with respect to the centre of the element $(\xi_*^{\mathrm{T}} = \{0,0,0\})$:

$$\begin{aligned}\boldsymbol{P}^{\mathrm{h}} &\approx \widetilde{\boldsymbol{P}}(\boldsymbol{H}_0^{\mathrm{h}}) + \frac{\partial \widetilde{\boldsymbol{P}}(\boldsymbol{H}^{\mathrm{h}})}{\partial \boldsymbol{H}^{\mathrm{h}}}\left(\left.\frac{\partial \boldsymbol{H}^{\mathrm{h}}}{\partial \xi}\right|_{\xi=\boldsymbol{0}} \xi + \left.\frac{\partial \boldsymbol{H}^{\mathrm{h}}}{\partial \eta}\right|_{\xi=\boldsymbol{0}} \eta + \left.\frac{\partial \boldsymbol{H}}{\partial \zeta}\right|_{\xi=\boldsymbol{0}} \zeta \right) \\ &= \boldsymbol{P}_0^{\mathrm{h}} + \boldsymbol{A}_0^{\mathrm{h}}\left(\boldsymbol{j}_0^{\mathrm{l}}\, \boldsymbol{L}_{\mathrm{hg}}^{\mathrm{l}}\, \boldsymbol{M}_{\mathrm{hg}}\, \boldsymbol{U}_{\mathrm{e}} + \boldsymbol{j}_0^{\mathrm{l}}\, \boldsymbol{L}_{\mathrm{enh}}\, \boldsymbol{W}_{\mathrm{e}}\right)\end{aligned} \tag{3}$$

The hourglass stabilization part can be evaluated analytically, i.e. a numerical integration procedure is not needed, the element requires only one Gauss point. In contrast, the solid-shell element is based on a Taylor expansion of $\boldsymbol{P}^{\mathrm{h}}$ with respect to the point $(\xi_*^{\mathrm{T}} = \{0,0,\zeta\})$, i.e. the Gauss points in this element lie on the normal with respect to the shell midsurface through the element centre.

$$\begin{aligned}\boldsymbol{P}^{\mathrm{h}} &\approx \widetilde{\boldsymbol{P}}\left(\boldsymbol{H}_*^{\mathrm{h}}\right) + \frac{\partial \widetilde{\boldsymbol{P}}\left(\boldsymbol{H}^{\mathrm{h}}\right)}{\partial \boldsymbol{H}^{\mathrm{h}}}\left(\left.\frac{\partial \boldsymbol{H}^{\mathrm{h}}}{\partial \xi}\right|_{\xi=\xi_*} \xi + \left.\frac{\partial \boldsymbol{H}^{\mathrm{h}}}{\partial \eta}\right|_{\xi=\xi_*} \eta \right) \\ &= \boldsymbol{P}_*^{\mathrm{h}} + \boldsymbol{A}_*^{\mathrm{h}}\left(\left(\boldsymbol{j}_0^{\mathrm{l}}\, \boldsymbol{L}_{\mathrm{hg}*}^{\mathrm{l}} + \boldsymbol{j}_0^{2}\, \boldsymbol{L}_{\mathrm{hg}*}^{2}\right)\boldsymbol{M}_{\mathrm{hg}}\, \boldsymbol{U}_{\mathrm{e}} + \boldsymbol{j}_0^{\mathrm{l}}\, \boldsymbol{L}_{\mathrm{enh}*}\, \boldsymbol{W}_{\mathrm{e}}\right)\end{aligned} \tag{4}$$

Using the 3D one-Gauss point concept, no enhanced variables have to be *explicitly* determined. We finally solve the non-linear equation $\boldsymbol{R}_0(\boldsymbol{U}) + \boldsymbol{K}_{\mathrm{stab}}\,\boldsymbol{U} - \boldsymbol{F}_{\mathrm{ext}} = \boldsymbol{0}$ where $\boldsymbol{R}_0(\boldsymbol{U})$ is the global residual force vector evaluated in the centre of the element and $\boldsymbol{K}_{\mathrm{stab}}$ denotes the global hourglass stabilization matrix. $\boldsymbol{U}$ is the global nodal displacement vector and $\boldsymbol{F}_{\mathrm{ext}}$ the vector of external loading. On the other hand, the shell element formulation requires to determine three internal element variables (connected to the enhanced strain). We arrive at the equation system

$$\boldsymbol{R}_{\zeta}\left(\boldsymbol{U},\boldsymbol{W}\right) + \boldsymbol{K}_{\mathrm{stab}}\,\boldsymbol{U} - \boldsymbol{F}_{\mathrm{ext}} = \boldsymbol{0}, \quad \boldsymbol{R}_{\mathrm{we}}\left(\boldsymbol{U}_{\mathrm{e}},\boldsymbol{W}_{\mathrm{e}}\right) = \boldsymbol{0}\,. \tag{5}$$

The index ζ indicates that here a numerical integration procedure over the thickness direction ζ has to be performed.

2.2 Model adaptive concept

The principle idea is to use as few elements as possible over the thickness. In thin undamaged structures where the assumption "plane cross-section" is approximately fulfilled a discretisation with only one element over the thickness might be sufficient. In massy or damaged regions where warping is not negligible the number of elements must be noticeably higher. Obviously a suitable error criterion is needed to automate the procedure. In the present paper we use a criterion formulated in terms of the leading bending component of the elastic left Cauchy-Green strain tensor $(\mathbf{b}_{\mathrm{e}})_{11}$. A plane cross-section means that the bending strain is linearly distributed over the cross-section. The stronger the warping the larger is the deviation of the distribution of $(\mathbf{b}_{\mathrm{e}})_{11}$ from this linear function. Accordingly the error criterion is formulated as the sum of deviations from the linearly interpolated strains of the outer Gauss points (cp. Fig. 1).

Starting from an initial configuration of several elements in longitudinal but only one solid-shell element with e.g. 16 Gauss points in thickness direction the error criterion is checked after every converged load step. If it is violated the element is cut in half and a “hanging node” is introduced. The hanging node concept serves to connect regions with different numbers of elements over the thickness. Consequently the degrees-of-freedom at the hanging nodes have to be coupled to the nodal displacements of the adjacent element.

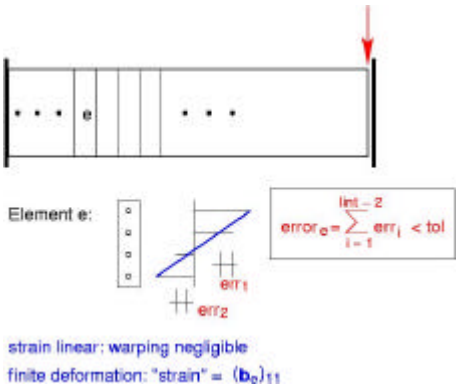

Fig. 1: Geometry and error criterion

The coupling conditions have an effect on the residual force vector as well as on the tangential stiffness matrix. This is consi- dered after the assembling procedure. After the discretisation is adopted the time step has to be repeated. If no further refinement is possible the solid–shell elements are substituted by the computationally more efficient continuum elements.

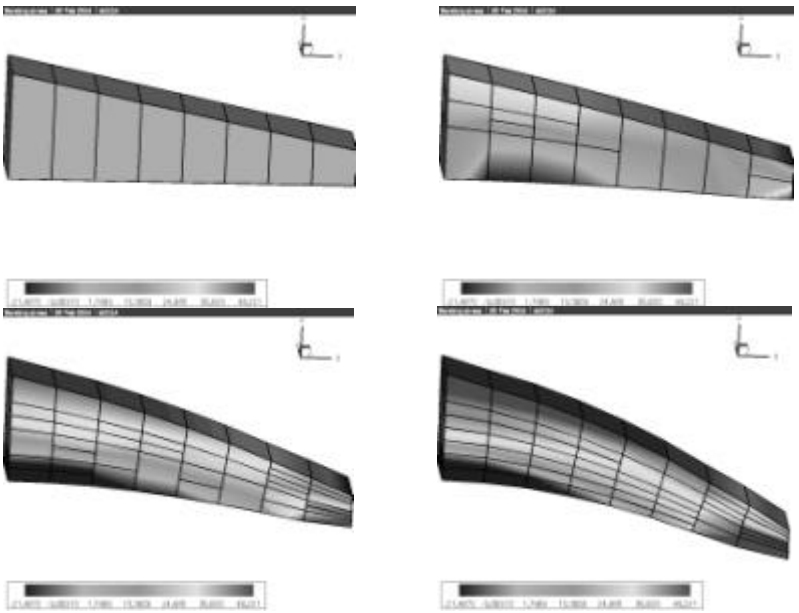

Fig. 2: “Hanging node” adaptivity

As numerical example we look at a clamped beam structure (see also Fig. 1). The system is loaded by a vertical displacement at the right side. The initial configuration consists of eight Q1SP solid-shell elements arranged in longitudinal direction. The material is non-linearly elasto-plastic. In Fig. 2 the adaptive refinement procedure is visualised. As expected the mesh refines itself in massy and strongly stressed zones, i.e. in the parts with larger thickness and in the loading area.

Subsequently a study of convergence has been carried out. In this context we compare the results of the model adaptive concept (MODA) with the ones achieved with a homogeneous mesh refinement (8/1, 8/2, 8/4 elements). The first number refers to the number of elements in the longitudinal direction, the second to the number of elements in thickness direction. In Fig. 3 we work with the Q1SP solid-shell concept as it has been presented in the above, i.e. with enhanced degrees-of-freedom. The formulation is then well suitable for thick structures. This is shown in Fig. 3.

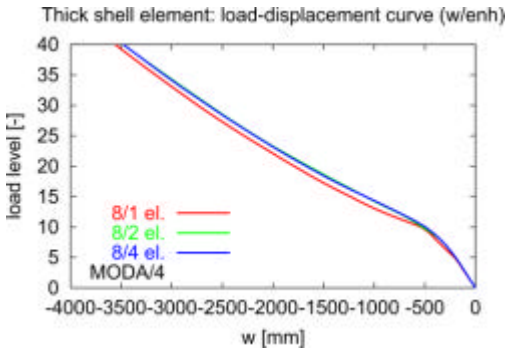

Fig. 3: convergence study *with* the enhanced element formulation

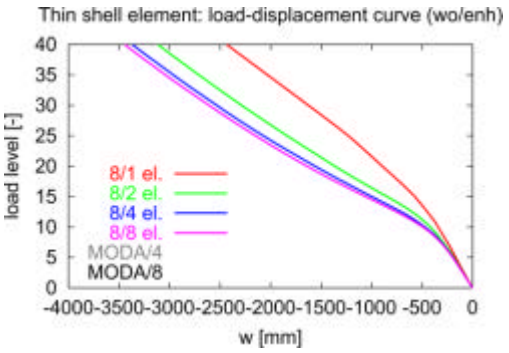

Fig. 4: convergence study *without* the enhanced element formulation

Obviously the differences between the results of MODA and the computation with two or four elements over the thickness are marginal. MODA finds automatically the converged solution. Neglecting the enhanced degrees-of-freedom in Q1SP leads to a shell formulation which exhibits locking for thick structures. However, it is still very appropiate for thin structures. The thin shell element has been used for the study on the right side (Fig. 4), where much larger differences between the computations with 1, 2, 4 and 8 elements over the thickness are observed. It is now even more clearly visible that MODA refines accordingly. For large displacements the solution with 8/8 elements is recovered.

3 Model reduction via truncated balanced realisation (TBR)

In the framework of system theory many approaches have been developed (Antoulas, Sorensen and Gugerin 2001) to reduce large-scale dynamical systems. One of them is the system theoretical method of truncated balanced realisation (TBR) which is based on the fundamental paper of (Moore 1981). This serves as basis for many other balanced model reduction methods as e.g. positive real balancing, stochastic balancing, LQG balancing or frequency weighted balanced reduction (cp. e.g. (Van Gestel, De Moor, Anderson and VanOverschee 2001), (Ober and Fuhrmann 1993)) and has been extended to nonlinear problems by e.g. (Lall, Marsden and Glavaški 2002). Meanwhile the method is well-developed for the model reduction of linear systems and appears in standard text books such as (Dullerud and Paganini 2000). Other authors apply this system theoretical approach on mechanical systems e.g. (Schemann and Smith 1998).

The here suggested concept is also based on the work of (Moore 1981). The transfer to physical coordinates is achieved via the procedure of (Yae and Inman 1999). Our goal is to apply the method to large dynamical systems. To circumvent numerical difficulties we divide the component which shall be reduced into small subsystems. After the model reduction we reassemble the substitute model in state space form by a novel substructure technique which will be discussed in what follows.

3.1 Truncated balanced realisation (TBR)

We start from the well-known equation of motion in which $\boldsymbol{M}$, $\boldsymbol{D}$, $\boldsymbol{K}$ and $\boldsymbol{B}_o$ denote the mass, damping, stiffness and input influence matrices.

$$\boldsymbol{M}\,\ddot{\boldsymbol{q}}(t) + \boldsymbol{D}\,\dot{\boldsymbol{q}}(t) + \boldsymbol{K}\boldsymbol{q}(t) = \boldsymbol{B}_o\boldsymbol{u}(t) \tag{6}$$

This equation is transformed into a first order differential equation called state space representation:

$$\dot{\boldsymbol{x}}(t) = \boldsymbol{A}\,\boldsymbol{x}(t) + \boldsymbol{B}\boldsymbol{u}(t) + \boldsymbol{B}_w\,\boldsymbol{w}(t), \quad \boldsymbol{y}(t) = \boldsymbol{C}\,\boldsymbol{x}(t) + \boldsymbol{D}\,\boldsymbol{u}(t) + \boldsymbol{J}\,\boldsymbol{w}(t)$$

$$\boldsymbol{A} = \begin{bmatrix} -\boldsymbol{M}^{-1}\boldsymbol{D} & -\boldsymbol{M}^{-1}\boldsymbol{K} \\ \boldsymbol{I} & \boldsymbol{0} \end{bmatrix}, \quad \boldsymbol{B} = \begin{bmatrix} \boldsymbol{M}^{-1}\boldsymbol{B}_o \\ \boldsymbol{0} \end{bmatrix} \tag{7}$$

Whereas the state vector $\boldsymbol{x}^T(t) = \left\{ \boldsymbol{q}(t)^T,\ \boldsymbol{q}(t)^T \right\}$ includes n velocities and n displacements. $\boldsymbol{u}(t)$ contains the control force and $\boldsymbol{y}(t)$ is the vector of sensor measurements $(m \times 1)$. The matrix $\boldsymbol{A}$ is the $(2n \times 2n)$ state matrix; $\boldsymbol{B}$ is the $(2n \times m)$ input matrix and $\boldsymbol{C}$ ist the $(1 \times 2n)$ output matix. All kinds of disturbances are neglected in this approach ($\boldsymbol{B}_w = \boldsymbol{D} = \boldsymbol{J} = \boldsymbol{0}$).

The idea of the TBR method can be summed up in the following way: Starting from the system theoretical elementary properties of *controllability* and *observability* we look for a special coordinate transformation which leads to an equally controllable and observable system. This special state is called the "*internally balanced state*". In order to find this particular state the observability gramian $\boldsymbol{W}_o$ and the controllability gramian $\boldsymbol{W}_c$ have to be determined. For this purpose we solve the Lyapunov matrix equations $\boldsymbol{A}\boldsymbol{W}_c + \boldsymbol{W}_c\boldsymbol{A}^T + \boldsymbol{B}\boldsymbol{B}^T = \boldsymbol{0}$ and $\boldsymbol{A}^T\boldsymbol{W}_o + \boldsymbol{W}_o\boldsymbol{A}^T + \boldsymbol{C}^T\boldsymbol{C} = \boldsymbol{0}$. Subsequently these matrices are decomposed by a Cholesky decomposition according to $\boldsymbol{W}_o = \boldsymbol{L}_o\boldsymbol{L}_o^T$, $\boldsymbol{W}_c = \boldsymbol{L}_c\boldsymbol{L}_c^T$. The singular value decomposition $\boldsymbol{L}_o^T\boldsymbol{L}_c = \boldsymbol{U}\,\Sigma\,\boldsymbol{V}$ enables the computation of the balancing transformation matrix $\boldsymbol{T} = \boldsymbol{L}_c\,\boldsymbol{V}\,\Sigma^{-1/2}$. Applying the transformation $\boldsymbol{x} = \boldsymbol{T}\,\boldsymbol{x}_b$ leads to the balanced state described by the state space equation $\dot{\boldsymbol{x}}_b = \boldsymbol{A}_b\boldsymbol{x}_b + \boldsymbol{B}_b\,\boldsymbol{u}, \quad \boldsymbol{y} = \boldsymbol{C}_b\,\boldsymbol{x}_b$ in which the gramians $\boldsymbol{W}_{cb} = \boldsymbol{W}_{cb} = \Sigma = \mathrm{diag}(\sigma_1,\ldots,\sigma_{2n})$ are positive definite diagonal matrices. They contain the singular values in descending order. In this particular coordinate system the magnitude of the singular values indicates the influence of the single states on the system response. That means the least controllable and observable states of the system can be deleted. Afterwards the balanced-reduced system is transformed back into the physical coordinate system by deleting the corresponding rows and columns.

To demonstrate the efficiency of the modified TBR method a $1.6\,\mathrm{m}$ long, rectangular (thickness $t = 4.0\,\mathrm{cm}$ and height $h = 1.5\,\mathrm{cm}$) cantilever beam of steel (Young's modulus $E = 210000\ \mathrm{N/mm^2}$, $\rho = 7.85\ \mathrm{kg/dm^3}$) discretised by ten Bernoulli frame elements is reduced. A proportional damping matrix is calculated using for simplicity Rayleigh damping ($a = ß = 10^{-5}$).

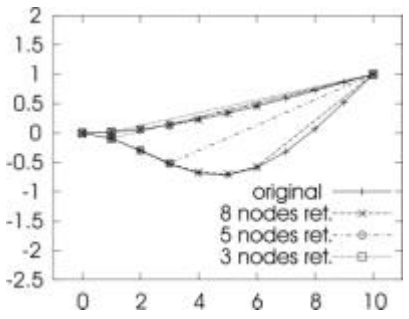

Fig. 5: Changes of the first and second mode shapes during the reduction

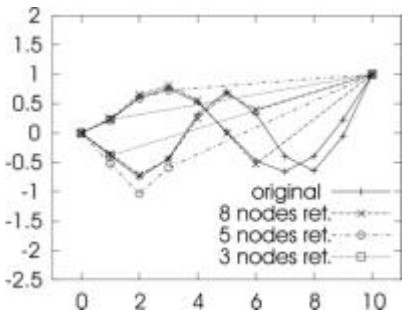

Fig. 6: Changes of the third and fourth mode shapes during the reduction

In Fig. 5 and 6 the first four mode shapes of the original unreduced beam are displayed. With the proposed method it is possible to delete physical degrees-of-freedom (rotations and displacements), or in other words, physical nodes. The procedure has important advantages if one intends to couple the reduced system to other structural components (which could be e.g.

discretised by means of the finite element method). We then define the “couple nodes” as “master nodes”. These are retained in the system whereas the other nodes (“slave nodes”) may be deleted. It is certainly unavoidable that the mode shapes are no longer modelled accurately. However, the eigenvector components at the master nodes and the eigenvalues are preserved qualitatively well (cp. Fig. 5 and Fig. 6).

4 Substructuring

In the field of structural dynamics a significant amount of research has been invested in the coupling of substructures. (Dubigeon and Peseux 1994) deliver an overview about the existing techniques and introduce a classification by the boundaries of the substructures. They distinguish between “locked-boundary”, “free-boundary” and mixed methods. We propose here a substructuring technique which is valid for “locked” und “free” subsystems. Due to the unsupported coupling nodes this technique belongs to the methods of “free-boundary” substructures.

We present in this Section a new substructure technique for differential equation systems of second order and extend its applicability to differential equation systems of first order. The proposed procedure enables us to accomplish a parallel and dynamic computation of substructures in state space representation and to calculate the system response of the entire structure in physical coordinates.

4.1 Differential equation systems of second order

To explain the procedure at a simple example a beam structure is separated into two single substructures which are connected via a coupling force $\boldsymbol{P}^{\mathrm{C}}$ (cp. Fig. 7).

For each of the substructures the equation of motion is formulated in terms of the FE matrices $\boldsymbol{M}^{\mathrm{i}}$ (mass matrix), $\boldsymbol{K}^{\mathrm{i}}$ (stiffness matrix), $\boldsymbol{D}^{\mathrm{i}}$ (damping matrix):

$$\boldsymbol{M}^{\mathrm{i}}\,\ddot{\boldsymbol{q}}^{\mathrm{i}} + \boldsymbol{D}^{\mathrm{i}}\,\dot{\boldsymbol{q}}^{\mathrm{i}} + \boldsymbol{K}^{\mathrm{i}}\,\boldsymbol{q}^{\mathrm{i}} = \boldsymbol{P}^{\mathrm{i}} \pm \boldsymbol{P}^{\mathrm{C}} \tag{8}$$

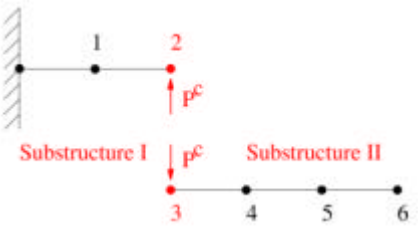

Fig. 7: Decomposed structure

The vector of external loads $\boldsymbol{P}^{\mathrm{i}}$ is modified by the coupling force vector $\boldsymbol{P}^{\mathrm{C}}$. Each of the equations of motion can be discretised by any time discretisation procedure e.g. by means of the Newmark scheme:

$$\begin{aligned}
&\boldsymbol{K}^{\mathrm{i}}_{\mathrm{eff}}\,\boldsymbol{q}^{\mathrm{i}}_{\mathrm{n+1}} = \boldsymbol{P}^{\mathrm{i}}_{\mathrm{eff}}\left(\boldsymbol{P}^{\mathrm{C}}\right), \qquad \boldsymbol{K}^{\mathrm{i}}_{\mathrm{eff}} = \frac{1}{\beta\,(\Delta t)^2}\boldsymbol{M}^{\mathrm{i}} + \frac{\gamma}{\Delta t}\boldsymbol{D}^{\mathrm{i}} + \boldsymbol{K}^{\mathrm{i}} \\
&\boldsymbol{P}^{\mathrm{i}}_{\mathrm{eff}} = \boldsymbol{P}^{\mathrm{i}}_{\mathrm{n+1}} + \boldsymbol{M}^{\mathrm{i}}\left[\frac{1}{\beta\,(\Delta t)^2}\,\boldsymbol{q}_{\mathrm{n}} + \frac{1}{\beta\,\Delta t}\,\dot{\boldsymbol{q}}_{\mathrm{n}} + \frac{1-2\beta}{2\beta}\,\ddot{\boldsymbol{q}}_{\mathrm{n}}\right] + \boldsymbol{D}^{\mathrm{i}}\left[\frac{\gamma}{\beta\,\Delta t}\boldsymbol{q}_{\mathrm{n}} + \frac{\gamma-\beta}{\beta}\,\dot{\boldsymbol{q}}_{\mathrm{n}} + \frac{\gamma-2\beta}{2\beta}\,\ddot{\boldsymbol{q}}_{\mathrm{n}}\right]
\end{aligned} \tag{9}$$

Corresponding to the coupling forces $\boldsymbol{P}^{\mathrm{C}}$ the compatibility conditions $\boldsymbol{q}^{\mathrm{C,I}}_{\mathrm{n+1}} = \boldsymbol{q}^{\mathrm{C,II}}_{\mathrm{n+1}}$ have to be fulfilled at the coupling nodes. More precisely, the degrees-of-freedom at the coupling nodes of

the subsystems have to be identical.The timely discretised equations together with the compatibility conditions yield an equation system for the coupling forces $\boldsymbol{P}^{\mathrm{C}}$ which can be evaluated. Finally the response of the entire system is computed without assembling the subsystems.

4.2 State space representation

4.2.1 Unreduced systems

As presented in Section 3 the TBR method results in reduced systems in state space representation. So the proposed substructure technique has to be adopted to first order differential equation systems.

Starting again from the equations of motion of the subsystems (8) the mass matrices $\boldsymbol{M}^{\mathrm{i}}$ are lumped and split in such a way that each subsystem contains the complete coupling nodal mass at the coupling node.

$$\boldsymbol{M}^{\mathrm{C}} = \boldsymbol{M}^{\mathrm{CI}} + \boldsymbol{M}^{\mathrm{CII}}, \qquad \boldsymbol{M}^{\mathrm{I}} = \left[\begin{array}{c|c} \boldsymbol{M}_{\mathrm{r}}^{\mathrm{I}} & \\ \hline & \boldsymbol{M}^{\mathrm{C}} \end{array}\right] \qquad \boldsymbol{M}^{\mathrm{II}} = \left[\begin{array}{c|c} \boldsymbol{M}_{\mathrm{r}}^{\mathrm{II}} & \\ \hline & \boldsymbol{M}^{\mathrm{C}} \end{array}\right] \tag{10}$$

Now each equation of motion is transformed into the state space representation by the multiplication with $\left[\boldsymbol{M}^{\mathrm{C}}\right]^{-1}$ from the left. This leads to a modified unity matrix:

$$\boldsymbol{E}_{\mathrm{mod}}^{\mathrm{CI}} = \left[\boldsymbol{M}^{\mathrm{C}}\right]^{-1} \boldsymbol{M}^{\mathrm{CI}} \quad \boldsymbol{E}_{\mathrm{mod}}^{\mathrm{CII}} = \boldsymbol{M}^{\mathrm{CII}} = \left[\boldsymbol{M}^{\mathrm{C}}\right]^{-1} \boldsymbol{M}^{\mathrm{CI}}, \quad \boldsymbol{E}_{\mathrm{mod}}^{\mathrm{I}} = \left[\begin{array}{c|c} \boldsymbol{I} & \\ \hline & \boldsymbol{E}^{\mathrm{CI}} \end{array}\right] \quad \boldsymbol{E}_{\mathrm{mod}}^{\mathrm{II}} = \left[\begin{array}{c|c} \boldsymbol{I} & \\ \hline & \boldsymbol{E}^{\mathrm{CII}} \end{array}\right] \tag{11}$$

The resulting unreduced modified first line of the state space representations (12) are assembled in a way analogously to the proposed procedure for differential equation systems of second order (Sec. 4.1).

$$\boldsymbol{E}_{\mathrm{mod}}^{\mathrm{i}}\, \ddot{\boldsymbol{q}}^{\mathrm{i}} + \left[\boldsymbol{M}_{\mathrm{mod}}^{\mathrm{i}}\right]^{-1} \boldsymbol{D}^{\mathrm{i}}\, \dot{\boldsymbol{q}}^{\mathrm{i}} + \left[\boldsymbol{M}_{\mathrm{mod}}^{\mathrm{i}}\right]^{-1} \boldsymbol{K}^{\mathrm{i}}\, \boldsymbol{q}^{\mathrm{i}} = \left[\boldsymbol{M}_{\mathrm{mod}}^{\mathrm{i}}\right]^{-1} \boldsymbol{P}^{\mathrm{i}} \pm \left[\boldsymbol{M}_{\mathrm{mod}}^{\mathrm{i}}\right]^{-1} \boldsymbol{P}^{\mathrm{C}} \tag{12}$$

4.2.2 Reduced systems

In the following we discuss the combination of the coupling procedure with model reduction (see e.g. Fig 8). Hereby we assume that the coupling node does not belong to the reduced part of subsystem II. This is because for the coupling procedure the nodal mass of the coupling node has to be known before and after the reduction. Furthermore, at least the mass matrix of the coupling node has to be lumped.

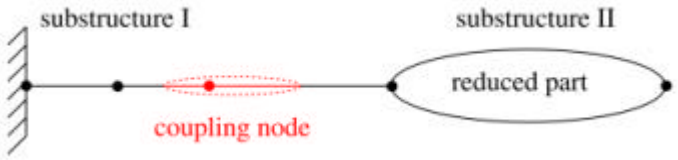

Fig. 8: Coupling of TBR reduced systems

The TBR procedure reduces the state space matrix $\boldsymbol{A}$ of the substructure II which is indicated by the index “r” (see eq. (13)). The index “C” denotes the coupling node which is not affected by the reduction.

$$\begin{bmatrix} \ddot{\boldsymbol{q}}_{\mathrm{r}} \\ \boldsymbol{E}_{\mathrm{mod}}^{\mathrm{C\,II}}\,\ddot{\boldsymbol{q}}^{\mathrm{C}} \\ \dot{\boldsymbol{q}}_{\mathrm{r}} \\ \dot{\boldsymbol{q}}^{\mathrm{C}} \end{bmatrix} = \underbrace{\begin{bmatrix} -\left[\boldsymbol{M}_{\mathrm{r}}^{\mathrm{II}}\right]^{-1}\boldsymbol{D}_{\mathrm{r}}^{\mathrm{II}} & -\left[\boldsymbol{M}_{\mathrm{r}}^{\mathrm{II}}\right]^{-1}\boldsymbol{D}^{\mathrm{IIC}} & -\left[\boldsymbol{M}_{\mathrm{r}}^{\mathrm{II}}\right]^{-1}\boldsymbol{K}_{\mathrm{r}}^{\mathrm{II}} & -\left[\boldsymbol{M}_{\mathrm{r}}^{\mathrm{II}}\right]^{-1}\boldsymbol{K}^{\mathrm{IIC}} \\ -\left[\boldsymbol{M}^{\mathrm{C}}\right]^{-1}\boldsymbol{D}^{\mathrm{C\,II}} & -\left[\boldsymbol{M}^{\mathrm{C}}\right]^{-1}\boldsymbol{D}^{\mathrm{C}} & -\left[\boldsymbol{M}^{\mathrm{C}}\right]^{-1}\boldsymbol{K}^{\mathrm{C\,II}} & -\left[\boldsymbol{M}^{\mathrm{C}}\right]^{-1}\boldsymbol{K}^{\mathrm{C}} \\ \mathbf{I} & \mathbf{0} & \mathbf{0} & \mathbf{0} \\ \mathbf{0} & \mathbf{I} & \mathbf{0} & \mathbf{0} \end{bmatrix}}_{\boldsymbol{A}_{\mathrm{r}}} \begin{bmatrix} \dot{\boldsymbol{q}}_{\mathrm{r}} \\ \dot{\boldsymbol{q}}^{\mathrm{C}} \\ \boldsymbol{q}_{\mathrm{r}} \\ \boldsymbol{q}^{\mathrm{C}} \end{bmatrix} + \begin{bmatrix} \left[\boldsymbol{M}_{\mathrm{r}}^{\mathrm{II}}\right]^{-1}\boldsymbol{P}_{\mathrm{r}}^{\mathrm{II}} \\ \left[\boldsymbol{M}^{\mathrm{C}}\right]^{-1}\boldsymbol{P}^{\mathrm{C}} \\ \mathbf{0} \\ \mathbf{0} \end{bmatrix} \quad (13)$$

The rectangular coupling matrices, subscripted by both indices “C” and “II”, are unknown after the reduction and have to be identified. Under the assumptions that Rayleigh damping is used and that at least the mass matrices of the coupling node are lumped ($\boldsymbol{D}^{\mathrm{C\,II}} = ß\ \boldsymbol{K}^{\mathrm{C\,II}}$) the second line of (13) is rewritten (14) and rearranged (15):

$$\boldsymbol{E}_{\mathrm{mod}}^{\mathrm{C\,II}}\,\ddot{\boldsymbol{q}}^{\mathrm{c}} = -\left[\boldsymbol{M}^{\mathrm{C}}\right]^{-1}\boldsymbol{D}^{\mathrm{C\,II}}\dot{\boldsymbol{q}}_{\mathrm{r}} - \left[\boldsymbol{M}^{\mathrm{C}}\right]^{-1}\boldsymbol{D}^{\mathrm{C}}\dot{\boldsymbol{q}}^{\mathrm{C}} - \left[\boldsymbol{M}^{\mathrm{C}}\right]^{-1}\boldsymbol{K}^{\mathrm{C\,II}}\boldsymbol{q}_{\mathrm{r}} - \left[\boldsymbol{M}^{\mathrm{C}}\right]^{-1}\boldsymbol{K}^{\mathrm{C}}\boldsymbol{q}^{\mathrm{C}} + \left[\boldsymbol{M}^{\mathrm{C}}\right]^{-1}\boldsymbol{P}^{\mathrm{C}} \quad (14)$$

$$\boldsymbol{E}_{\mathrm{mod}}^{\mathrm{C\,II}}\,\ddot{\boldsymbol{q}}^{\mathrm{C}} + \left[\boldsymbol{M}^{\mathrm{C}}\right]^{-1}\boldsymbol{D}^{\mathrm{C}}\,\dot{\boldsymbol{q}}^{\mathrm{C}} + \left[\boldsymbol{M}^{\mathrm{C}}\right]^{-1}\boldsymbol{K}^{\mathrm{C}}\,\boldsymbol{q}^{\mathrm{C}} - \left[\boldsymbol{M}^{\mathrm{C}}\right]^{-1}\boldsymbol{P}^{\mathrm{C}} = \boldsymbol{P}^{\mathrm{C}*} = -\left[\boldsymbol{M}^{\mathrm{C}}\right]^{-1}\boldsymbol{K}^{\mathrm{C\,II}}\left(\beta\dot{\boldsymbol{q}}_{\mathrm{r}} + \boldsymbol{q}_{\mathrm{r}}\right) \quad (15)$$

The resulting under-determined equation system (15) is not sufficient to identify $\boldsymbol{K}^{\mathrm{C\,II}}\left(\mathrm{i\ x\ j}\right)$. Herein i is the number of coupling conditions and j is the dimension of the reduced subsystem II. For this reason the vector $\left(\beta\dot{\boldsymbol{q}}_{\mathrm{r}} + \boldsymbol{q}_{\mathrm{r}}\right)$ $\left(\mathrm{j\ x\ 1}\right)$ shall be extended to a regular matrix by the following procedure. If we assume that i coupling conditions exist ($\boldsymbol{P}^{\mathrm{C}*}$ (i x 1)) and the reduced substructure has j degrees-of-freedom, j displacement and load vectors are needed. After these data sets habe been determined the relation (15) is transferred into the equation (16).

$$\left[\boldsymbol{M}^{\mathrm{C}}\right]^{-1}\boldsymbol{K}^{\mathrm{C\,II}} = -\boldsymbol{P}^{\mathrm{C}*}\left(\beta\,\dot{\boldsymbol{Q}}_{\mathrm{r}} + \boldsymbol{Q}_{\mathrm{r}}\right)^{-1} \quad (16)$$

An analogous procedure (with i known states) applied to the first line of (13) leads to $\left[\boldsymbol{M}_{\mathrm{r}}\right]^{-1}\boldsymbol{K}^{\mathrm{IIC}} = -\boldsymbol{P}^{\mathrm{II}*}\left(\beta\,\dot{\boldsymbol{Q}}^{\mathrm{C}} + \boldsymbol{Q}^{\mathrm{C}}\right)^{-1}$. To collect the data sets for the variables $\ddot{\boldsymbol{q}}_{\mathrm{unred}}$, $\dot{\boldsymbol{q}}_{\mathrm{unred}}$, $\boldsymbol{q}_{\mathrm{unred}}$ and the load states $(\boldsymbol{M}_{\mathrm{red}}^{\mathrm{II}})^{-1}\boldsymbol{P}_{\mathrm{unred}}^{\mathrm{II}}$ the required number of time steps $(\max\{\mathrm{i, j}\})$ are computed at the unreduced system. They are modified according to the TBR method by transforming them into the “balanced state”

$$\boldsymbol{x}_{\mathrm{b}} = \boldsymbol{T}^{-1}\,\boldsymbol{x} = \boldsymbol{T}^{-1}\begin{bmatrix} \dot{\boldsymbol{q}}_{\mathrm{r,unred}} \\ \boldsymbol{q}_{\mathrm{r,unred}} \end{bmatrix}, \qquad \boldsymbol{B}_{\mathrm{b}} = \boldsymbol{T}^{-1}\,\boldsymbol{B} = \boldsymbol{T}^{-1}\begin{bmatrix} \left(\boldsymbol{M}_{\mathrm{r}}^{-1}\,\boldsymbol{P}_{\mathrm{r}}\right)_{\mathrm{unred}} \\ \boldsymbol{0} \end{bmatrix}. \quad (17)$$

After the truncation they are pulled back to the physical coordinate system.

$$\boldsymbol{x}_{\mathrm{r}} = \begin{bmatrix} \dot{\boldsymbol{u}}_{\mathrm{r}} \\ \boldsymbol{u}_{\mathrm{r}} \end{bmatrix} = \boldsymbol{T}^{-1}\,\boldsymbol{x}_{\mathrm{br}}\,, \qquad \boldsymbol{B}_{\mathrm{r}} = \begin{bmatrix} \boldsymbol{M}_{\mathrm{r}}^{-1}\,\boldsymbol{P}_{\mathrm{r}} \\ \mathbf{0} \end{bmatrix} = \boldsymbol{T}^{-1}\,\boldsymbol{B}_{\mathrm{br}} \quad (18)$$

4.3 Numerical Examples

The proposed methodology is applied to an arch of the Münster Hiltruper bridge (Fig. 9) to assess the quality and the feasibility of the coupling and reduction procedure.

The geometry and material properties are summerised in Tab. 1. The subsystem I is the one where damage is assumed to occur. Therefore it is not reduced. To model the material behavior more accurately we choose a finer discretisation than in the other parts of the construction.

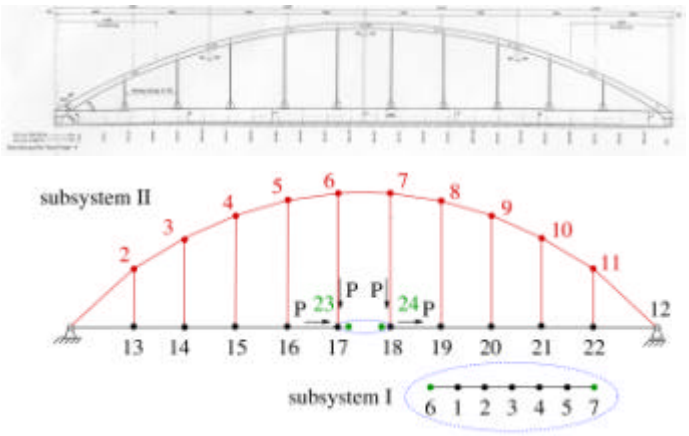

Fig. 9: Arch of the Münster Hiltruper bridge

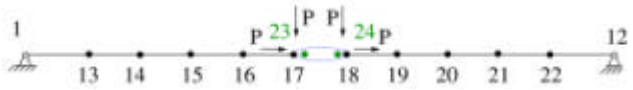

Fig. 10: Reduced substructre II of the Münster Hiltruper bridge

The slightly damped subsystem II is reduced by the TBR method up to almost 50% (the entire upper part is condensed, see Fig. 10). As provided in Tab. 1 hardly any error in the first four eigenvalues is found.

del. node numbers	λ_1	λ_2	λ_3	λ_4	del. nodes [%]
-	0.577657	1.946305	6.348856	6.451507	-
5 - 8	0.577658	1.946267	6.348858	6.451500	18
3 - 10	0.577657	1.946307	6.348855	6.451506	36
2 - 11	0.577662	1.946304	6.348856	6.451507	**45**

Tab. 1: First four eigenvalues of the reduced structure

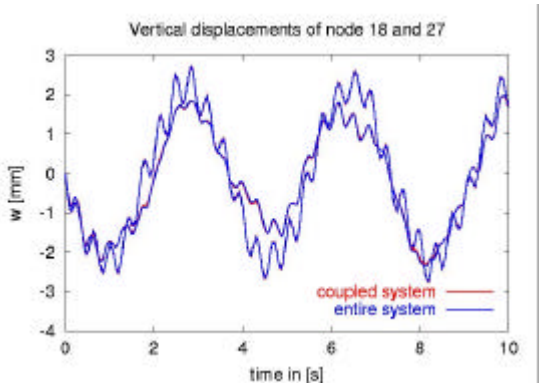

Fig. 11: System response of the entire and the coupled system of the Münster Hiltruper bridge

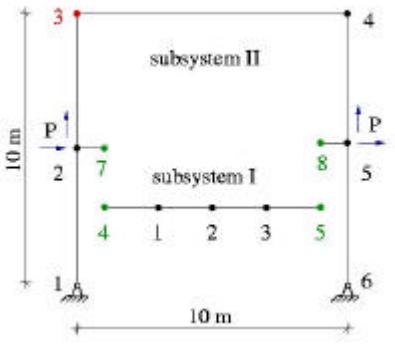

Fig. 12: Frame structure

Using the procedure outlined in (10) - (12) both substructures are coupled in the state space representation. In Fig. 11 the vertical displacements of node 18 and 3 (node 27 in the entire structure) of the entire and the coupled structure are compared and show a good match. That means that the described coupling procedure shows quite good results.

In a second example (see Fig. 12) the coupling and reduction strategy is applied to a frame with $E = 2.1 \cdot 10^5\ \mathrm{N/mm^2}$, $\rho = 7.85\ \mathrm{kg/dm^3}$, $A = 21.1\ \mathrm{N/mm^2}$ and $I_y = 349.0\ \mathrm{cm^4}$. Fig. 13 shows

that the couple procedure is successful. Both curves have the same amplitude and almost the same frequencies. In a second step node 3 of the second subsystem (see Fig. 12) is deleted. The observed vertical displacement of node 2 (Fig. 14) for the coupled/reduced and the coupled/unreduced system are identical.

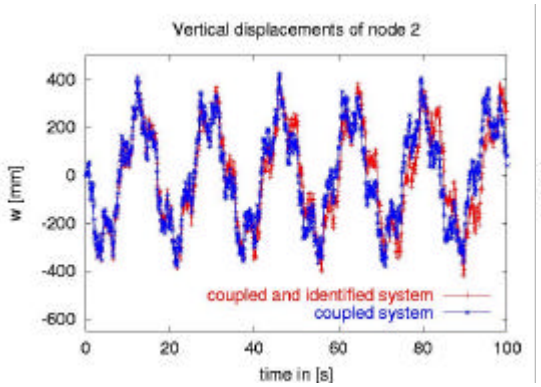

Fig. 13: System response of the coupled and the coupled and identified system

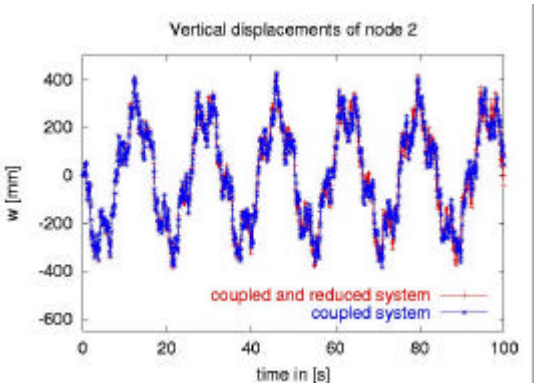

Fig. 14: System response of the coupled and the coupled/reduced system

5 Conclusions

In this paper a novel model adaptive concept is presented. The innovative and robust algorithm combines the advantages of the hourglass stabilised Q1SP element family with the "hanging node" concept. The automatic mesh adaption in thickness direction controlled by a warping error criterion is demonstrated for large inelastic deformations. In the second part the system theoretical TBR model reduction method is applied to more complex mechanical systems. Its effectiveness and robustness has been enhanced by a novel substructure technique. One important advantage of the suggested concept is that the reduction is achieved with respect to physically relevant quantities.

6 References

Antoulas A.C., D.C. Sorensen and S. Gugercin. 2001. Structured matrices in operator theory, numerical analysis, control, signal and image processing.Contemporary Mathematics. AMS publications.

Barbone, P.E., D. Givoli and I. Patlashenko. 2003. Optimal modal reduction of vibrating substructures. International Journal for Numerical Methods in Engineering 57: 341-69.

Belytschko, T. and W. Bachrach. 1986. Efficient implementation of quadrilaterals with high coarse-mesh accuracy. Computer Methods in Applied Mechanics and Engineering 54: 279-301

Belytschko, T. and L.P. Bindemann. 1991. Assumed strain stabilisation of the eight-node hexahedral element. Computer Methods in Applied Mechanics and Engineering 105: 225-60

Belytschko, T., J. S.-J. Ong, W.K. Liu and J.M. Kennedy. 1984. Hourglass control in linear and nonlinear problems. Computer Methods in Applied Mechanics and Engineering 43: 251-76

Cardoso, R.P.R. J.-W. Yoon, J.J. Grácio, F. Barlat and J.M.A. César de Sá. 2002. Development of a one point quadrature shell element for nonlinear applications with contact and anisotropy. Computer Methods in Applied Mechanics and Engineering 191: 5177-206.

Dubigeon, S. and B. Peseux. 1994. Dynamic condensation: The free mode methode. International Journal for Numerical Methods in Engineering 37: 3521-43.

Dullerud, G. and F. Paganini. 2000. *Course in robust control theory: a convex approach.* Berlin: Springer.

Lall, S., J. Marsden and S. Glavaški. 2002. A subspace approach to balanced truncation for model reducation of nonlinear control systems. International Journal of Robust and nonlinear Control 12: 519-35.

Legay, A. and A. Combescure. 2003. Elastoplastic stability analysis of shells using the physically stabilized finite element SHB8PS. International Journal for Numerical Methods in Engineering 57: 1299-1322.

Moore, B.. 1981. Principal component analysis in linear systems: controllability, observability and model reduction. IEEE Transactions on Automatic Control 26(1): 17-32.

Ober, R. and P.R. Fuhrmann. 1993. A functional approach to LQG balancing. International Journal of Control: 57(3).

Puso, M.A.. 2000. A highly efficient enhanced assumed strain physically stabilized hexahedral element. International Journal for Numerical Methods in Engineering 49: 1029-64.

Petersmann, N.. Substrukturtechnik und Kondensation bei der Schwingungsanalyse, VDI Fortschrittsberichte, Reihe 11, Nr. 76.

Reese, S. 2003. On a consistent hourglass stabilization techniq ue to treat large inelastic deformations and thermo-mechanical coupling in plane strain problems. submitted to Int. J. Numer. Meth. Engng 57:1095-1127.

Reese, S. 2004. On a physically stabilised one point finite element formulation for three-dimensional finite elasto-plasticity. submitted to CMAME.

Schemann, A.G. and H.A. Smith. 1998. Vibration control of cable-stayed bridges - part 1: modeling issues. Earthquake Engineering and Structural Dynamics 27: 811-24.

Simo, J.C. and F. Armero. 1992. Geometrically nonlinear enhanced strain mixed methods and the method of incompatible modes. Computer Methods in Applied Mechanics and Engineering 110: 359-66.

Simo, J.C. and M.S. Rifai. 1990. A class of mixed assumed strain methods and the method of incompatible modes. International Journal for Numerical Methods in Engineering 29: 1595-1638

Soize, C.. Dynamic Substructuring in the Medium-Frequency Range. AIAA Journal 41(6): 1113-18

Van Gestel, T., B. de Moor, B. Anderson and P. van Overschee. 2001. On frequency weighted balanced truncation: Hankel singular values and error bounds. European Journal of Control 7: 584-92.

Wriggers, P. and S. Reese. 1996. A note on enhanced strain methodsfor large deformations. Computer Methods in Applied Mechanics and Engineering 135: 201-9.

Yae, K.H. and D.J. Inman. 1999.Techniques in control- oriented reduction of finite element modeling in structural dynamic systems. In *Structural Dynamic Systems Computational Techniques and Optimization: Dynamic Analysis and Control Techniques.1-54*. 14th ed. Amsterdam: Gordon and Breach Science Publishers.